Applied Physics Letters ARTICLE scitation.org/journal/apl

Measurement of the temperature dependence of mechanical losses induced by an electric field in undoped silicon disk resonators

Cite as: Appl. Phys. Lett. **122**, 142109 (2023); doi: 10.1063/5.0143587
Submitted: 24 January 2023 · Accepted: 7 March 2023 ·
Published Online: 6 April 2023

View Online Export Citation CrossMark

Y. Yu. Klochkov and V. P. Mitrofanov[a)]

AFFILIATIONS

Faculty of Physics, Lomonosov Moscow State University, 119991 Moscow, Russia

Note: This paper is part of the APL Special Collection on Gravitational Wave Detectors.
[a)]**Author to whom correspondence should be addressed:** vpmitrofanov@physics.msu.ru

ABSTRACT

Test masses of future laser interferometric gravitational-wave detectors will be made of high-purity silicon and cooled, in particular, to 123 K in the LIGO Voyager project. Electrostatic actuators are supposed to be used to tune the test mass position. Capacitive coupling of the actuator electrodes with the silicon test mass results in the mechanical loss caused by electric currents flowing in silicon having a finite resistivity. This loss is a cause of additional thermal noise. In this study, we present the results of temperature dependence of the electric field induced loss in the bending vibration mode of commercial disk-shaped undoped silicon wafers in the temperature range of 100–295 K.

Cooling the test masses of future laser interferometric gravitational-wave (GW) detectors makes it possible to reduce their thermal noise and increase the sensitivity of the detectors. In one of the possible design options of the LIGO Voyager, Einstein Telescope, and Cosmic Explorer concepts, test masses of detectors will be made of high-purity monocrystalline silicon and cooled to low temperatures.[1–3] In LIGO Voyager, the silicon test masses will be operated near 123 K. Near this temperature, the thermal expansion coefficient of silicon crosses zero, thermoelastic loss and noise are drastically reduced, as well as thermoelastic distortions of the mirror surface. High-purity silicon is needed in order to reduce optical absorption at wavelengths of about 2000 nm.[1]

In currently operating GW detectors, the fused silica test masses exhibit electrostatic charge buildup from a variety of mechanisms.[4] The interaction between these charges and the environment, as well as the electric field of the electrostatic actuator, can generate force noise on the test masses.[5–9] Electric charges may also build up on the silicon test masses of future detectors.[10] The silicon test masses and suspension elements have the advantage of being conductive, which makes them easier to discharge. However, the conductivity of the silicon test masses implies that charges move to reorganize in response to oscillations under an electric field, creating additional mechanical loss and associated thermal noise.

Disk mechanical resonators are widely used to study mechanical losses in multilayer high reflectivity thin film optical coatings deposited on the test masses of current and next-generation GW detectors.[11,12] The nodal support technique is used to suppress the loss due to the support.[13] Mechanical losses caused by an electric field in silicon disk resonators at room temperature were studied in Ref. 14. A model that relates the electric field induced mechanical loss in disk resonator to the resistivity of the material was proposed. It follows from the model that, under certain conditions that are satisfied for the silicon resonators under study, the electric field induced loss Q_E^{-1} is directly proportional to the resistivity of silicon. In this paper, we present the results of measurement of mechanical losses induced by an electric field in undoped silicon disk resonators in the temperature range of 100–295 K.

As resonators, we used commercial (UniversityWafer, Inc) double side polished silicon ⟨100⟩ wafers with a diameter of 50.8 mm and a thickness of 0.28 mm. Two flats with length of 16 and 8 mm were cut into opposite sides of the wafer. The primary flat of the longest length is aligned with the [110] direction in the silicon crystal structure. The secondary flat indicates the wafer surface orientation and doping of the wafer. For an undoped silicon wafer, the location of the secondary flat parallel to the primary one indicates ⟨100⟩ orientation. According to the manufacturer's specification, these undoped silicon wafers had resistivity $\rho > 10\,\mathrm{k\Omega\,cm}$. The wafer was clamped between two duralumin tips with a hemispherical surface pressed into polyoxymethylene stems, which were inserted into duralumin sleeves mounted in a duralumin frame as shown in Fig. 1(a). The bottom stem was mounted in a spring-loaded manner. The measurements were also carried out with

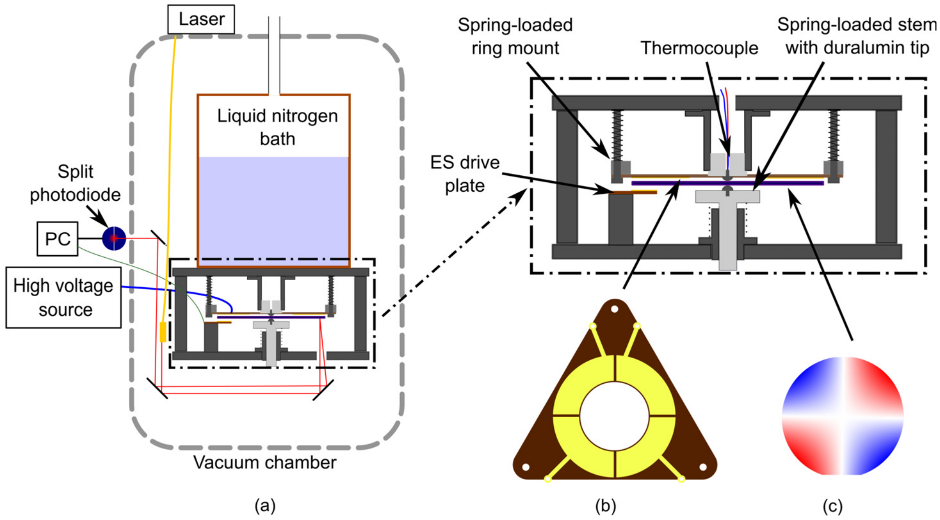

FIG. 1. (a) Schematic of the experimental setup. (b) Fiberglass copper clad plate with etched and gold-plated electrode. (c) Shape of the wafer vibration mode.

tips made of brass and coated with indium. Their results were similar to those obtained with duralumin tips, which are presented below. The temperature of the wafer was measured using a copper–constantan thermocouple attached to the top tip. The wafer was grounded through contact with the top tip. The frame was attached to a copper vessel mounted inside the vacuum chamber and filled with liquid nitrogen. A plate with a ring-shaped electrode divided into four sectors was located over the silicon wafer. The electrode was etched on a fiberglass copper clad plate and gold-plated [Fig. 1(b)]. A separation gap of about 0.2–0.3 mm between the wafer and the electrode plate was adjusted using three spring-loaded screws. The gap size was determined measuring the capacitance between the wafer and the electrode sectors. The wafer bending vibration mode with two nodal diameters ($f \approx 830$ Hz) was excited resonantly using an electrostatic drive. The calculated distribution of the displacement in a direction orthogonal to the surface for this mode is shown by the color in Fig. 1(c).

The wafer vibration was monitored using the optical sensor. The laser beam reflected from the vibrating wafer passed through a system of mirrors and was detected by a split quadrant photodiode placed outside the vacuum chamber.[15] Custom-developed software based on LabVIEW was used to monitor the mode resonant frequency f and the decay time τ from the photodiode signal measured during the wafer free vibration decay. The mechanical loss Q^{-1} was calculated from the relation $Q^{-1} = (\pi f \tau)^{-1}$.

The electric field induced mechanical loss Q_E^{-1} was determined as a difference between Q_U^{-1} measured when a DC voltage U was applied between the wafer and the electrode and Q_0^{-1} measured when the electrode was grounded,

$$Q_E^{-1} = Q_U^{-1} - Q_0^{-1}. \tag{1}$$

The results of the study of room temperature mechanical loss caused by an electric field in the silicon disk resonator vibrating on the bending mode with two nodal diameters were presented in Ref. 14. It was shown that, under certain conditions (satisfied for the silicon resonators under study), the electric field induced loss Q_E^{-1} is directly proportional to the silicon resistivity ρ and the relative frequency shift to the power of 4/3, which is caused by a negative stiffness introduced into the oscillating wafer by an electric field between it and a nearby electrode,[14]

$$Q_E^{-1} \propto \left(\frac{\Delta f}{f_0}\right)_E^{4/3}. \tag{2}$$

Measurements of the temperature dependence of losses in a silicon wafer were mainly carried out with natural cooling of the wafer after pouring liquid nitrogen into a vessel inside the vacuum chamber. The average wafer cooling rate was about 2 K/min at 280 K and 0.4 K/min at 120 K. For control purposes, some measurements were carried out with natural heating, but they were time consuming. The measurements could be carried out in two regimes. In the first one, the loss was first measured as a function of temperature when the wafer was cooled from 295 to 100 K in the absence of an electric field (the wafer and the electrode were grounded). Then the measurements were repeated when a DC voltage U was applied between the electrode and the wafer. The electric field induced loss Q_E^{-1} was calculated according to Eq. (1) for selected values of the wafer's temperature. In the second regime, we alternated loss measurements with and without an electric field while the wafer was cooling. The results of measurements were approximated so that it was possible to subtract the loss measured without the electric field from the loss measured with the field and, thus, calculate the temperature dependence of the loss induced by the electric field. We mainly used the second regime, since it is less affected by a drift, which is mainly due to the thermal expansion.

Thermal expansion effects on the fastening elements of the wafer and electrode led to a change in the gap between them during cooling. We controlled the change in the gap, measuring the change in the electric field induced shift of the wafer vibration mode frequency. It was found that during cooling, the size of the gap changed by no more than $\pm 5\%$. After reinstalling the wafer, when the size of the gap between the wafer and the electrode inevitably changed, we corrected the measured loss value, bringing it to the same gap using the measured electric field induced frequency shift in accordance with Eq. (2).

The mechanical loss of the undoped silicon wafer vibration mode measured with the electric field off is shown as black squares in

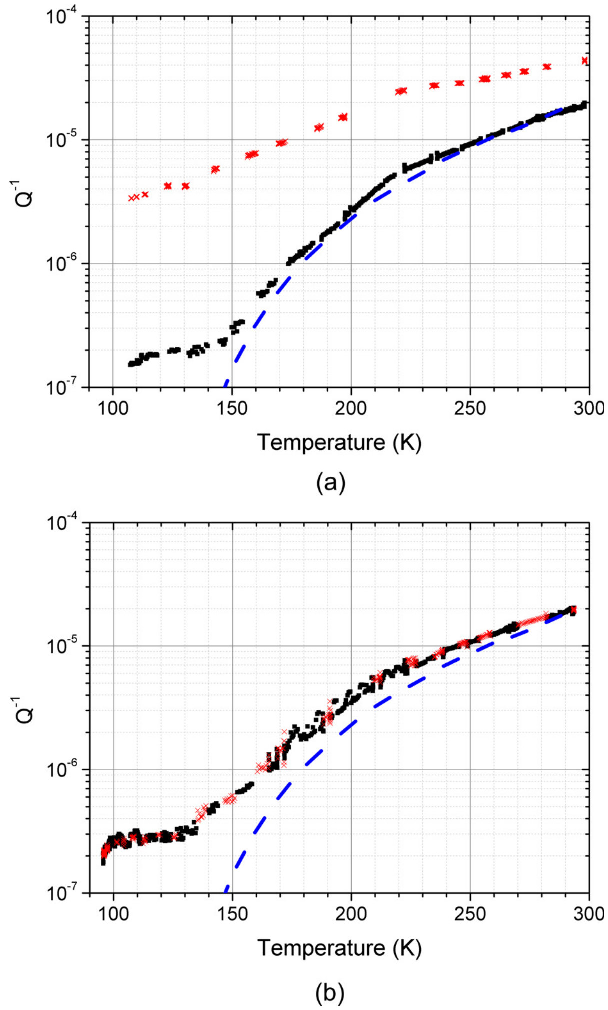

FIG. 2. Temperature dependences of the mechanical loss of the wafer vibration mode measured without an electric field (black squares), measured with DC voltage $U = 150\,\mathrm{V}$ applied between the wafer and the electrode (red crosses) for the undoped silicon wafer (a) and for the boron doped silicon wafer with small resistivity (b). The calculated thermoelastic loss is shown by the blue dashed line.

Fig. 2(a). The thermoelastic loss of this mode calculated using the COMSOL Multiphysics FEM package[16] is shown by the blue dashed line. The temperature dependent thermodynamic parameters of silicon were taken from Refs. 17 and 18. It can be seen that the dominant loss mechanism at temperatures above approximately 200 K is consistent with the thermoelastic loss.[19] At lower temperatures, the thermoelastic loss is suppressed due to the approach to zero of the thermal expansion coefficient, and the main contribution to the observed loss can be the losses in the clamping of the wafer and the surface losses.[20] The mechanical loss of the undoped silicon wafer vibration mode measured with a DC voltage $U = 150\,\mathrm{V}$ applied between the wafer and the electrode is shown as red crosses.

It is interesting to compare the presented data for the wafer made of undoped silicon with similar data obtained from measurements of the loss of the vibration mode of the wafer made of boron doped silicon [$\rho = (1.0 \pm 0.5)\,\Omega\,\mathrm{cm}$], which are shown in Fig. 2(b). In this wafer, Ohmic loss, being directly proportional to the resistivity of silicon, is more than 10 000 times less in the undoped wafer. This is clarified in Fig. 2(b), due the negligible difference between the measurements with and without electric field in particular, in the temperature range near 120 K. We can conclude that losses induced by the electric field in the measured vibrational mode of silicon wafers, but not due to silicon resistivity, do not exceed the value 1×10^{-7} in the temperature range near 120 K.

When measuring the loss and frequency shift caused by the electric field in the vibration mode of the undoped silicon wafer, it was found that, starting from the temperature of about 200 K and lower, transient responses with times exceeding 1 s occur when the DC electric field is turned on and off (see Fig. 3). They manifested themselves both when measuring the frequency shift and the loss caused by the electric field. The frequency shift is determined by the electric field, which arises when the capacitance between the wafer and the electrode is charged through the contact metal–semiconductor. Parameters of the transients depended on the magnitude and sign of the voltage applied between the wafer and the electrode. With decreasing temperature, the duration of transients increased. The influence of the change in the sign of the applied voltage can be explained by the fact that the electrical contact between duralumin and undoped silicon forms a rectifying Schottky barrier.[21] In our case, it corresponds to contact with n-type semiconductor. It follows from the calculation of the resistive loss and frequency shift induced by an electric field that they are directly proportional to the square of the applied voltage.[14] For the linearization of the effect, time dependence of square root was constructed from the values of the frequency shift. The result is shown in Fig. 3(e). The structure of the transient responses to switching on and off the field becomes almost the same, consisting of two parts, which may be due to the influence of the surface states of silicon on the processes in the contact. Note that for undoped silicon wafers, we observed noticeable transients upon cooling below about 200 K and did not observe them above these temperatures. Whereas for doped low-resistivity silicon wafers, no noticeable transients were observed in the entire range of temperatures under study. In order to eliminate the influence of transients on the results of measuring losses in the undoped silicon wafer, we applied the DC forward voltage of 150 V to the electrode, and the loss measurements began after the end of transients. So the transients had little effect on the measurement results. They reflected the properties of the electrical contact between the silicon wafer and its grounding metal conductor. The formation of a high quality grounding electrical contact with silicon is not an easy task.[22] This must be taken into account when developing the low-noise suspension of silicon test masses for future cryogenic GW detectors.

To investigate the reproducibility of the measurements, the undoped silicon wafer was repeatedly cooled and heated several times within two months without opening the vacuum chamber. The temperature dependences of the electric field induced mechanical loss Q_{Er}^{-1} reduced to the same gap of 0.22 mm between the wafer and the electrode obtained for several series of measurements, which are shown in Fig. 4. The time-dependent behavior of measured losses was observed at temperatures from about 200 to 295 K, while at lower temperatures, the data scatter was significantly reduced. This is important for the use of electrostatic actuators in future GW detectors with cooled silicon test masses. To estimate the resistivity of undoped silicon, from which

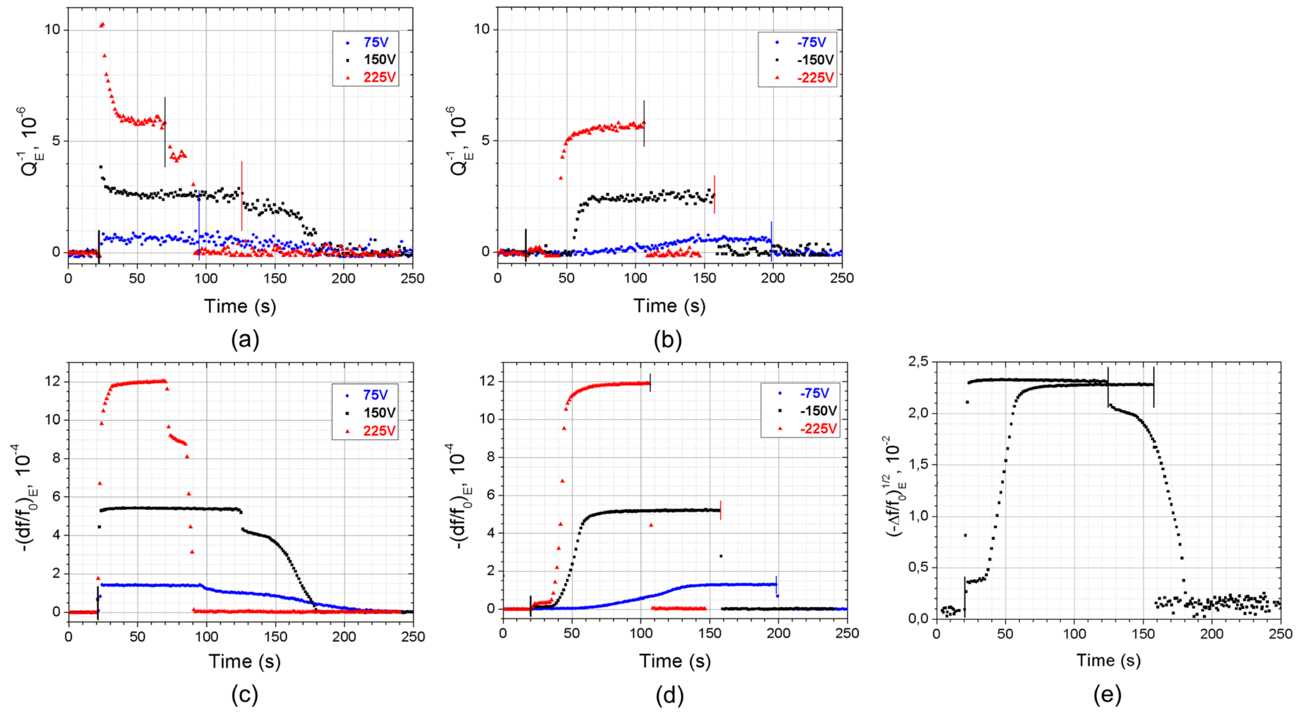

FIG. 3. Transient responses of the field induced loss (a) and (b) and the resonant frequency shift (c) and (d) to turn on and off the DC voltage. Square root of the field induced resonant frequency shift transient response to turn on and off DC voltage $U = \pm 150$ V—forward and reverse (e). $T \approx 100$ K.

the wafer was made, we used the relation that relates the loss of the corresponding vibration mode of the disk silicon resonator to the silicon resistivity.[14] The resistivity ρ was found to be (27 ± 5) kΩcm at 293 K, which corresponds to a phosphorus impurity concentration of 1.6×10^{11} cm^{-3}. For this impurity concentration, the temperature dependence of silicon resistivity was calculated using the resistivity calculator.[23] The calculated dependence is shown with an error band in

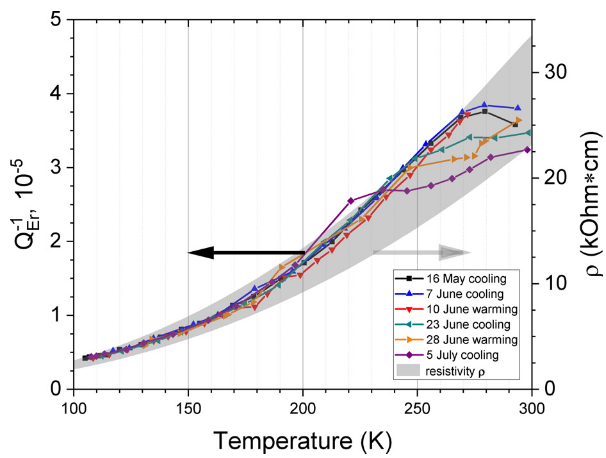

FIG. 4. Temperature dependences of the electric field induced mechanical loss Q_{Er}^{-1} reduced to the same gap of 0.22 mm between the wafer and the electrode obtained for several series of measurements (left Y-axis). Calculated temperature dependence of silicon resistivity shown with an error band (right Y-axis).

Fig. 4. Such a behavior of the low-doped silicon resistivity is explained by an increase in the mobility of charge carriers upon cooling in the investigated temperature range.[24,25] The time-dependent behavior of the measured loss can be associated with the silicon resistivity changes. The time-dependence of resistivity was observed at room temperature in high-resistivity silicon wafers.[26] The authors associated this time-dependence of the resistivity with the presence of thin native oxide layers on silicon surface and trapped charges at the Si/SiO_2 interface.[27] Additional surface electrical conductance, which changes the measured resistivity of silicon, is carried out through these interface states and depends on their filling. Our measurement has shown that the scatter of the data decreased at lower temperatures. We assume that the conduction through the interface states is carried out according to the same mechanism of the thermally activated hopping conductance through the surface states of silicon in which the surface conductance decreases with decreasing temperature.[28]

In conclusion, we have measured the mechanical loss of the bending vibration mode of an undoped silicon wafer caused by a DC electric field applied between the wafer and the nearby electrode in the temperature range of 100–295 K. The loss induced by the electric field was observed to be directly proportional to the silicon resistivity, as expected.[14] The resistivity of lightly doped silicon in the investigated temperature range decreases with decreasing temperature due to an increase in the mobility of charge carriers. Our measurements have shown that the mechanical loss follows this decrease in resistivity, with general agreement between calculations and experiment.

We also observed two different time-dependent behaviors of mechanical losses in undoped silicon wafers. First, the time-dependent behavior of measured losses has been observed at temperatures from about 200 to 295 K, while at lower temperatures, the data scatter was significantly reduced. The time-dependent behavior of the measured loss can be associated with the silicon resistivity changes caused by effect of interface states. Second, below temperatures of about 200 K, a transient response was observed when the DC voltage was switched on and off. We associate this behavior with the properties of the electrical contact between the silicon wafer and metal tip used for the wafer clamping and grounding. This transient behavior can have an impact on the design of electrostatic actuators for GW detectors using silicon test masses.

Any increase in mechanical losses of the silicon test masses leads to an increase in their thermal noise. The studies carried out make it possible to set acceptable parameters of electrostatic actuators used to adjust the position of the test masses of future GW detectors. The time-dependent behavior of the loss can be a source of excess noise, which requires further research.

The authors thank colleagues from the LIGO/Virgo/KAGRA (LVK) Collaboration for fruitful discussions. Authors are also grateful to Kirill Tokmakov for his help and Edgard Bonilla for the valuable comments. This research was supported by the Interdisciplinary Scientific and Educational School of Moscow University "Fundamental and Applied Space Research" and funded by the Russian Foundation for Basic Research under Project No. 19-29-11003. This paper has been assigned the LIGO DCC No. LIGO P-2300008-v2.

AUTHOR DECLARATIONS

Conflict of Interest

The authors have no conflicts to disclose.

Author Contributions

Yaroslav Yu Klochkov: Conceptualization (supporting); Formal analysis (lead); Investigation (lead); Methodology (supporting); Writing – original draft (lead). **Valeriy P. Mitrofanov:** Conceptualization (lead); Formal analysis (supporting); Funding acquisition (lead); Investigation (supporting); Methodology (lead); Writing – review & editing (lead).

DATA AVAILABILITY

The data that support the findings of this study are available from the corresponding author upon reasonable request.

REFERENCES

[1]R. X. Adhikari, K. Arai, A. F. Brooks *et al.*, "A cryogenic silicon interferometer for gravitational-wave detection," Classical Quantum Gravity **37**, 165003 (2020).
[2]M. Punturo, M. Abernathy, F. Acernese *et al.*, "The Einstein Telescope: A third-generation gravitational wave observatory," Classical Quantum Gravity **27**, 194002 (2010).
[3]E. D. Hall, K. Kuns, J. R. Smith *et al.*, "Gravitational-wave physics with Cosmic Explorer: Limits to low-frequency sensitivity," Phys. Rev. D **103**, 122004 (2021).
[4]L. G. Prokhorov and J. Kissel, "Interaction of the ESD with electrical charges of the test masses in Advanced LIGO," No. LIGO-G1600699-v1, 2016.
[5]S. Rowan, S. Twyford, R. Hutchins, and J. Hough, "Investigations into the effects of electrostatic charge on the Q-factor of a prototype fused silica suspension for use in gravitational wave detectors," Classical Quantum Gravity **14**, 1537–1543 (1997).
[6]V. P. Mitrofanov, N. A. Styazhkina, and K. V. Tokmakov, "Damping of the test mass oscillations caused by multistrip electrostatic actuator," Phys. Lett. A **278**, 25–29 (2000).
[7]M. J. Mortonson, C. C. Vassiliou, D. J. Ottaway, D. H. Shoemaker, and G. M. Harry, "Effects of electrical charging on the mechanical Q of a fused silica disk," Rev. Sci. Instrum. **74**, 4840–4847 (2003).
[8]E. Bonilla, P. Giuliani, B. Lantz, and A. Buikema, "Method for electromechanical modeling of Johnson noise in Advanced LIGO," Classical Quantum Gravity **38**, 025014 (2021).
[9]P. Campsie, J. Hough, S. Rowan, and G. Hammond, "Measurement of noise created by fluctuating electrostatic charges on dielectric surfaces using a torsion balance," Classical Quantum Gravity **31**, 175007 (2014).
[10]See https://dcc.ligo.org/LIGO-T2100298/public for "Instrument Science White Paper 2021, LIGO Document: LIGO-T2100298-v2."
[11]G. Cagnoli, M. Lorenzini, E. Cesarini *et al.*, "Mode-dependent mechanical losses in disc resonators," Phys. Lett. A **382**, 2165–2173 (2018).
[12]G. Vajente, M. Fazio, L. Yang *et al.*, "Method for the experimental measurement of bulk and shear loss angles in amorphous thin films," Phys. Rev. D **101**, 042004 (2020).
[13]K. Numata, G. B. Bianc, N. Ohishi *et al.*, "Measurement of the intrinsic mechanical loss of low-loss samples using a nodal support," Phys. Lett. A **276**, 37–46 (2000).
[14]Y. Yu. Klochkov, L. G. Prokhorov, M. S. Matiushechkina *et al.*, "Using silicon disk resonators to measure mechanical losses caused by an electric field," Rev. Sci. Instrum. **93**, 014501 (2022).
[15]L. G. Prokhorov, V. P. Mitrofanov, B. Kamai *et al.*, "Measurement of mechanical losses in the carbon nanotube black coating of silicon wafers," Classical Quantum Gravity **37**, 015004–015016 (2020).
[16]See https://comsol.com/comsol-multiphysics for "COMSOL Multiphysics Simulation Software."
[17]P. D. Desai, "Thermodynamic properties of iron and silicon," J. Phys. Chem. Ref. Data **15**, 967–984 (1986).
[18]C. Y. Ho, R. W. Powell, and P. E. Liley, "Thermal conductivity of the elements," J. Phys. Chem. Ref. Data **1**, 279–421 (1972).
[19]R. Lifshitz and M. L. Roukes, "Thermoelastic damping in micro- and nanomechanical systems," Phys. Rev. B **61**, 5600–5609 (2000).
[20]Y. Yang, T. Ono, and M. Esashi, "Surface effects and high quality factors in ultrathin single-crystal silicon cantilevers," Appl. Phys. Lett. **77**, 3860–3862 (2000).
[21]E. H. Rhoderick, "The physics of Schottky barriers," J. Phys. D **3**, 1153–1169 (1970).
[22]H. Yu, M. Schaekers, K. Barla *et al.*, "Contact resistivities of metal-insulator-semiconductor contacts and metal-semiconductor contacts," Appl. Phys. Lett. **108**, 171602 (2016).
[23]See https://www.pvlighthouse.com.au/resistivity for calculation of the resistivity and the carrier mobilities of a semiconductor based on the dopant concentration and temperature.
[24]S. S. Li and W. R. Thurber, "The dopant density and temperature dependence of electron mobility and resistivity in n-type silicon," Solid-State Electron. **20**, 609–616 (1977).
[25]J. Krupka, J. Breeze, A. Centeno *et al.*, "Measurements of permittivity, dielectric loss tangent, and resistivity of float-zone silicon at microwave frequencies," IEEE Trans. Microwave Theory Tech. **54**, 3995–4001 (2006).
[26]M. Li, S. Chen, Y. Liu *et al.*, "Investigation on time-dependent behavior of resistivity in high-resistivity silicon wafers," Mater. Sci. Semicond. Process. **151**, 106995 (2022).
[27]G. J. Gerardi, E. H. Poindexter, and P. J. Caplan, "Interface traps and P_b centers in oxidized (100) silicon wafers," Appl. Phys. Lett. **49**, 348–352 (1986).
[28]T. Tanikawa, K. Yoo, I. Matsuda *et al.*, "Nonmetallic transport property of the Si(111)7 $\times$ 7 surface," Phys. Rev. B **68**, 113303 (2003).